Article

DFT Study on Chemical N Fixation by Using a Cubane-Type RuIr S Cluster: Energy Profile for Binding and Reduction of N to Ammonia via Ru#N#NH (*x* = 1#3) Intermediates with Unique Structures

Hiromasa Tanaka, Hiroyuki Mori, Hidetake Seino,
Masanobu Hidai, Yasushi Mizobe, and Kazunari Yoshizawa

J. Am. Chem. Soc., **2008**, 130 (28), 9037-9047 • DOI: 10.1021/ja8009567 • Publication Date (Web): 18 June 2008

J|A|C|S
ARTICLES

Published on Web 06/18/2008

DFT Study on Chemical N_2 Fixation by Using a Cubane-Type $RuIr_3S_4$ Cluster: Energy Profile for Binding and Reduction of N_2 to Ammonia via Ru−N−NH_x ($x = 1-3$) Intermediates with Unique Structures

Hiromasa Tanaka,[†] Hiroyuki Mori,[‡] Hidetake Seino,[‡] Masanobu Hidai,[§] Yasushi Mizobe,*[,‡] and Kazunari Yoshizawa*[,†]

Institute for Materials Chemistry and Engineering, Kyushu University, Fukuoka 819-0395, Japan, Institute of Industrial Science, The University of Tokyo, Tokyo 153-8505, Japan, and Department of Materials Science and Technology, Faculty of Industrial Science and Technology, Tokyo University of Science, Noda, Chiba 278-8510, Japan

Received February 7, 2008; E-mail: kazunari@ms.ifoc.kyushu-u.ac.jp (K.Y.); ymizobe@iis.u-tokyo.ac.jp (Y.M.)

Abstract: The N−N bond activation of the dinitrogen ligand in the cubane-type mixed-metal sulfido cluster, $[(Cp^*Ir)_3\{Ru(tmeda)(N_2)\}(\mu_3\text{-}S)_4]$ (tmeda = $Me_2NCH_2CH_2NMe_2$), is investigated by using DFT calculations at the B3LYP level of theory. The elongated N−N bond distance, red-shifted N−N stretching, and negatively charged N_2 ligand indicate that the dinitrogen is reductively activated by complexation. The degree of the N−N bond activation is classified into the "moderately activated" category, [Studt, F.; Tuczek, F. *J. Comput. Chem.* 2006, 27, 1278] as in the Mo−triamidoamine complex that can catalyze N_2 reduction [Yandulov, D. V.; Schrock, R. R. *Science* 2003, 301, 76]. Availability of the $RuIr_3S_4$ cluster as a catalyst for N_2 reduction is discussed by optimizing possible intermediates in a catalytic cycle analogous to that proposed by Yandulov and Schrock. A calculated energy profile of the catalytic cycle demonstrates that the $RuIr_3S_4$ cluster can transform dinitrogen into ammonia in the presence of lutidinium cation and Cp^*_2Co as proton and electron sources, respectively. The $RuIr_3S_4$ clusters with an NNH_x ($x = 1-3$) ligand, which are intermediates in the catalytic cycle, have a significantly bent Ru−N−N linkage, although precedent NNH_x complexes generally adopt a linear M−N−N array. The unique structures of the nitrogenous ligands in these intermediates are interpreted in terms of the bonding interaction between the hydrogen atom bonded to the N_2 ligand and the adjacent iridium atom in the cuboidal $RuIr_3S_4$ framework.

1. Introduction

The reduction of inert dinitrogen to yield ammonia (nitrogen fixation) under ambient conditions is one of the most important and challenging topics in chemistry and biology.[1] This process involves difficulty in breaking the strong N≡N triple bond of dinitrogen, so that the industrial nitrogen fixation, i.e. the Haber−Bosch process, is attained only under drastic reaction conditions of high pressures and high temperatures. On the other hand, in the biological N_2-fixing system, enzyme nitrogenase transforms dinitrogen into ammonia under ambient conditions.[2] A recent X-ray crystallographic study of the Mo-containing nitrogenase revealed that its active site to reduce dinitrogen contains a metal sulfido cluster, the iron molybdenum cofactor (FeMo-co),[3] which has an $MoFe_7S_9X$ core consisting of two incomplete cubane-type units of $MoFe_3S_3$ and Fe_4S_3 bridged by three μ_2-sulfido ligands as well as a μ_6-X atom. The light atom X located at the center of the trigonal-prismatic cavity is presumed to be either N, O, or C but has not yet been identified. As for where dinitrogen is bound in FeMo-co and how dinitrogen is transformed into ammonia, only limited experimental information is accessible at present. Hence, a number of theoretical research studies have been done for the proposal of reliable mechanisms of nitrogen fixation in the enzyme.[4,5]

The other versatile approach to elucidate the mechanism of nitrogen fixation in nitrogenase is to synthesize metal sulfido clusters ligating nitrogenous substrates as models of its active site and investigate the coordination modes and reactivities of substrate molecules.[6] For example, Coucouvanis and co-workers demonstrated that cubane-type MFe_3S_4 (M = Mo, V) clusters

[†] Kyushu University.
[‡] The University of Tokyo.
[§] Tokyo University of Science.

(1) (a) MacKey, B. A.; Fryzuk, M. D. *Chem. Rev.* **2004**, *104*, 385–401. (b) Schlögl, R. *Angew. Chem., Int. Ed.* **2003**, *42*, 2004. (c) Shaver, M. P.; Fryzuk, M. D. *Adv. Synth. Catal.* **2003**, *345*, 1061. (d) Rees, D. C.; Howard, J. B. *Curr. Opin. Chem. Biol.* **2000**, *4*, 559.
(2) (a) Rees, D.; Tezcan, F. A.; Haynes, C. A.; Walton, M. Y.; Andrade, S.; Einsle, O.; Howard, J. B. *Philos. Trans. R. Soc. A* **2005**, *363*, 971. (b) Igarashi, R. Y.; Seefeldt, L. C. *Crit. Rev. Biochem. Mol. Biol.* **2003**, *38*, 351. (c) Burgess, B. K.; Lowe, D. J. *Chem. Rev.* **1996**, *96*, 2983. (d) Eady, R. R. *Chem. Rev.* **1996**, *96*, 3013. (e) Howard, J. B.; Rees, D. C. *Chem. Rev.* **1996**, *96*, 2965.
(3) Einsle, O.; Tezcan, F. A.; Andrade, S. L. A.; Schmid, B.; Yoshida, M.; Howard, J. B.; Rees, D. C. *Science* **2002**, *297*, 1696.
(4) (a) Dos Santos, P. C.; Dean, D. R.; Hu, Y.; Ribbe, M. W. *Chem. Rev.* **2004**, *104*, 1159. (b) Seefeldt, L. C.; Dance, I. G.; Dean, D. R. *Biochemistry* **2004**, *43*, 1401. (c) Barney, B. M.; Laryukhin, M.; Igarashi, R. Y.; Lee, H.-I.; Dos Santos, P. C.; Yang, T.-C.; Hoffman, B. M.; Dean, D. R.; Seefeldt, L. C. *Biochemistry* **2005**, *44*, 8030. (d) Barney, B. M.; McClead, J.; Lukoyanov, D.; Laryukhin, M.; Yang, T.-C.; Dean, D. R.; Hoffman, B. M.; Seefeldt, L. C. *Biochemistry* **2007**, *46*, 6784.

can catalyze the reduction of hydrazine (N_2H_4) into ammonia,[7] while Hidai, Mizobe, and co-workers reported the catalytic N−N bond cleavage of hydrazine by cubane-type $RuMo_3S_4$ and $Mo_2M_2S_4$ (M = Ir, Rh) clusters.[8] However, no metal sulfido clusters have been known that can bind or reduce N_2 in a well-defined manner[9] although the formation of some ammonia was claimed by the electroreduction of N_2 in the presence of $MoFe_3S_4$ clusters.[10]

With respect to transition metal complexes with dinitrogen as a ligand, significant progress has been made in the elucidation of the metal−N_2 bond. Since the discovery of the first transition metal−N_2 complex $[Ru(N_2)(NH_3)_5]^{2+}$ by Allen and Senoff in 1965,[11] a great number of well-defined N_2 complexes have been isolated for almost all d-block transition metals as well as some f-block metals.[12–16] These include the first molybdenum N_2 complex *trans*-$[Mo(N_2)_2(Ph_2PCH_2CH_2PPh_2)_2]$ reported by Hidai in 1969,[14] which proved later to undergo numerous transformations of its N_2 ligand by the studies of Hidai et al.[12a] and Chatt et al.,[12e,f] as well as the N_2 complexes with sulfur-donor ligands, e.g., mono- and dinuclear ruthenium−sulfur complexes prepared by Sellmann and co-workers that can bind not only N_2 but also N_2H_2, N_2H_4, and NH_3 under mild conditions.[15] The structures of these complexes provide useful insight into the binding mechanism of nitrogenous compounds in FeMo-co. For example, Reiher and co-workers have reported quantum chemical calculations to elucidate the activation mechanism of N_2 in Sellmann's complex as a model of FeMo-co.[17–20]

However, among the transition metal−N_2 complexes only a few have led to success in the catalytic conversion of N_2 into nitrogenous compounds. In 1989, Hidai, Mizobe, and co-workers reported that $[M(N_2)_2(PMe_2Ph)_4]$ (M = Mo, W) catalyzed the reaction of N_2 and Me_3SiCl to afford silylamines such as $N(SiMe_3)_3$ in the presence of Na.[21] More recently, in 2003, Yandulov and Schrock prepared $[Mo(N_2)(hiptN_3N)]$ (hiptN$_3$N = hexaisopropyl-terphenyl-triamidoamine) and demonstrated that N_2 was catalytically converted into ammonia in this Mo−triamidoamine system.[22–25] In their study, protons and electrons were supplied by 2,6-lutidinium tetrakis(3,5-bis(trifluoromethyl)phenyl)borate [LutH][BAr′$_4$] and decamethylchromocene Cp*$_2$Cr, respectively. Schrock's group also isolated and observed a number of intermediates in the reaction, leading to the proposal of a catalytic cycle (the so-called Yandulov−Schrock cycle) including alternating steps of protonation and reduction.[22] These excellent studies prompted computational approaches to clarify the mechanism of N_2 reduction in the Mo−triamidoamine system.[26–30] Cao and co-workers reported a DFT study on N_2 fixation in the Yandulov−Schrock cycle using a small model of the Mo complex, in which the hipt substituents were replaced by phenyl groups.[26] Studt and Tuczek investigated the energy profile of the Yandulov−Schrock cycle including a combination of proton/electron donors ($LutH^+$ and Cp*$_2$Cr) in the free enthalpy calculation.[27] Although they adopted a smaller model, in which the hipt substituents were replaced by hydrogen atoms, the calculation results indicated that all the reaction steps in the Yandulov−Schrock cycle are energetically downhill except for the first protonation to form a cationic diazenido complex. Reiher and co-workers performed detailed DFT calculations on the NH_3/N_2 exchange reaction in the Yandulov−Schrock cycle using a more realistic model, in which the hipt substituents are replaced by terphenyl groups,[28] and the real complex without any simplification.[29] They pointed out that simplification of the substituents in Schrock's complex must be considered with care and that oversimplification does not reliably reproduce the energetics of all steps of the catalytic cycle. Very recently

(5) (a) Kästner, J.; Blöchl, P. *J. Am. Chem. Soc.* **2007**, *129*, 2998. (b) Dance, I. *Biochemistry* **2006**, *45*, 6328. (c) Dance, I. *J. Am. Chem. Soc.* **2005**, *127*, 10925. (d) Siegbahn, P. E. M.; Westerberg, J.; Svensson, M.; Crabtree, R. J. *J. Phys. Chem. B* **1998**, *102*, 1615. (e) Huniar, U.; Ahlrichs, R.; Coucouvanis, D. *J. Am. Chem. Soc.* **2004**, *126*, 2588. (f) Schimpl, J.; Petrilli, H. M.; Blöchl, P. E. *J. Am. Chem. Soc.* **2003**, *125*, 15772. (g) Lovell, T.; Liu, T.; Case, D. A.; Noodleman, L. *J. Am. Chem. Soc.* **2003**, *125*, 8377. (h) Hinnermann, B.; Nørskov, J. K. *J. Am. Chem. Soc.* **2003**, *125*, 1466. (i) Deng, H. B.; Hoffmann, R. *Angew. Chem., Int. Ed. Engl.* **1992**, *32*, 1062.

(6) (a) Hidai, M.; Kuwata, S.; Mizobe, Y. *Acc. Chem. Res.* **2000**, *33*, 46. (b) Henderson, R. A. *Chem. Rev.* **2005**, *105*, 2365. (c) Ohki, Y.; Ikagawa, Y.; Tatsumi, K. *J. Am. Chem. Soc.* **2007**, *129*, 10457. (d) Ohki, Y.; Sunada, Y.; Honda, M.; Katada, M.; Tatsumi, K. *J. Am. Chem. Soc.* **2003**, *125*, 4052. (e) Lee, S. C.; Holm, R. H. *Chem. Rev.* **2004**, *104*, 1135.

(7) (a) Coucouvanis, D.; Demadis, K. D.; Malinak, S. M.; Mosier, P. E.; Tyson, M. A.; Laughlin, L. J. *J. Mol. Catal. A: Chem.* **1996**, *107*, 123. (b) Demadis, K. D.; Malinak, S. M.; Coucouvanis, D. *Inorg. Chem.* **1996**, *35*, 4038. (c) Malinak, S. M.; Demadis, K. D.; Coucouvanis, D. *J. Am. Chem. Soc.* **1995**, *117*, 3126.

(8) (a) Seino, H.; Masumori, T.; Hidai, M.; Mizobe, Y. *Organometallics* **2003**, *22*, 3424. (b) Takei, I.; Dohki, K.; Kobayashi, K.; Suzuki, T.; Hidai, M. *Inorg. Chem.* **2005**, *44*, 3768.

(9) (a) Kozlowski, P. M.; Shiota, Y.; Gomita, S.; Seino, H.; Mizobe, Y.; Yoshizawa, K. *Bull. Chem. Soc. Jpn.* **2007**, *80*, 2323. (b) Yoshizawa, K.; Kihara, N.; Shiota, Y.; Seino, H.; Mizobe, Y. *Bull. Chem. Soc. Jpn.* **2006**, *79*, 53. (c) Takei, I.; Kobayashi, K.; Dohki, K.; Nagao, S.; Mizobe, Y.; Hidai, M. *Chem. Lett.* **2007**, *36*, 546.

(10) Tanaka, K.; Hozumi, Y.; Tanaka, T. *Chem. Lett.* **1982**, 1203.

(11) (a) Allen, A. D.; Senoff, C. V. *Chem. Commun.* **1965**, 621. (b) Bottomley, F.; Nyburg, S. C. *Chem. Commun.* **1966**, 897. (c) Senoff, C. V. *J. Chem. Educ.* **1990**, *67*, 368.

(12) (a) Hidai, M.; Mizobe, Y. *Chem. Rev.* **1995**, *95*, 1115. (b) Pickett, C. J. *J. Biol. Inorg. Chem.* **1996**, *1*, 601. (c) Studt, F.; Tuczek, F. *J. Comput. Chem.* **2006**, *27*, 1278. (d) Neese, F. *Angew. Chem., Int. Ed.* **2006**, *45*, 196. (e) Chatt, J.; Dilworth, J. R.; Richards, R. L. *Chem. Rev.* **1978**, *78*, 589. (f) Henderson, R. A.; Leigh, G. H.; Pickett, C. J. *Adv. Inorg. Chem. Radiochem.* **1983**, *27*, 198.

(13) (a) Nishibayashi, Y.; Iwai, S.; Hidai, M. *Science* **1998**, *279*, 540. (b) Nishibayashi, Y.; Takemoto, S.; Iwai, S.; Hidai, M. *Inorg. Chem.* **2000**, *39*, 5946. (c) Hidai, M.; Mizobe, Y. *Pure Appl. Chem.* **2001**, *73*, 261.

(14) (a) Hidai, M.; Tominari, K.; Uchida, Y.; Misono, A. *Chem. Commun.* **1996**, 1392. (b) Hidai, M.; Tominari, K.; Uchida, Y. *J. Am. Chem. Soc.* **1972**, *94*, 110.

(15) (a) Sellmann, D.; Hautsch, B.; Rösler, A.; Heinemann, F. W. *Angew. Chem., Int. Ed.* **2001**, *40*, 1505. (b) Sellmann, D.; Hille, A.; Heinemann, F. W.; Moll, M.; Rösler, A.; Sutter, J.; Brehm, G.; Reiher, M.; Hess, B. A.; Schneider, S. *Inorg. Chim. Acta* **2003**, *348*, 194. (c) Sellmann, D.; Hille, A.; Rösler, A.; Heinemann, F. W.; Moll, M.; Brehm, G.; Schneider, S.; Reiher, M.; Hess, B. A.; Bauer, W. *Chem. Eur. J.* **2004**, *10*, 819.

(16) (a) Laplaza, C. E.; Cummins, C. C. *Science* **1995**, *268*, 861. (b) Saymore, S. B.; Brown, S. N. *Inorg. Chem.* **2006**, *45*, 9540.

(17) Reiher, M.; Sellmann, D.; Hess, B. A. *Theor. Chem. Acc.* **2001**, *106*, 379.

(18) Reiher, M.; Salomon, O.; Sellmann, D.; Hess, B. A. *Chem. Eur. J.* **2001**, *7*, 5195.

(19) Reiher, M.; Kirchner, B.; Hutter, J.; Sellmann, D.; Hess, B. A. *Chem. Eur. J.* **2004**, *10*, 4443.

(20) Kirchner, B.; Reiher, M.; Hille, A.; Hutter, J.; Hess, B. A. *Chem. Eur. J.* **2005**, *11*, 574.

(21) Komori, K.; Oshita, H.; Mizobe, Y.; Hidai, M. *J. Am. Chem. Soc.* **1989**, *111*, 1939.

(22) Yandulov, D. V.; Schrock, R. R. *Science* **2003**, *301*, 76.

(23) Schrock, R. R. *Acc. Chem. Res.* **2005**, *38*, 955.

(24) Yandulov, D. V.; Schrock, R. R.; Rheingold, A. L.; Ceccarelli, C.; Davis, W. M. *Inorg. Chem.* **2003**, *42*, 796.

(25) Yandulov, D. V.; Schrock, R. R. *Inorg. Chem.* **2005**, *44*, 1103.

(26) Cao, Z.; Zhou, Z.; Wan, H.; Zhang, Q. *Int. J. Quantum Chem.* **2005**, *103*, 344.

(27) Studt, F.; Tuczek, F. *Angew. Chem., Int. Ed.* **2005**, *44*, 5639.

(28) Le Guennic, B.; Kirchner, B.; Reiher, M. *Chem. Eur. J.* **2005**, *11*, 7448.

(29) Reiher, M.; Le Guennic, B.; Kirchner, B. *Inorg. Chem.* **2005**, *44*, 9640.

(30) Magistrato, A.; Robertazzi, A.; Carloni, P. *J. Chem. Theory Comput.* **2007**, *3*, 1708.

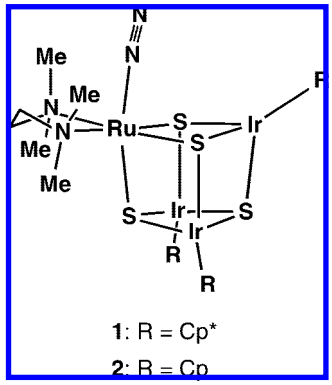

Figure 1. Structure of $[(RIr)_3\{Ru(tmeda)(N_2)\}(\mu_3\text{-}S)_4]$ **1** and **2** (**1**; R = Cp*, **2**; R = Cp).

Magistrato and co-workers have carried out extensive computations on the Yandulov−Schrock cycle using various DFT functionals and solvation models.[30] They presented that the energy profile of the catalytic cycle strongly depends on the exchange-correlation functional employed and the number of solvent molecules taken into account.

Recently Mizobe and co-workers succeeded in the isolation of the first cubane-type metal sulfido cluster having dinitrogen as a ligand: $[(Cp^*Ir)_3\{Ru(tmeda)(N_2)\}(\mu_3\text{-}S)_4]$ (**1**; Cp* = η^5-C_5Me_5) shown in Figure 1.[31] An X-ray crystallographic analysis revealed that the N_2 ligand in **1** coordinates at the Ru atom in an end-on manner. A characteristic N≡N stretching frequency observed at 2019 cm^{-1} is the lowest value among all Ru−N_2 complexes reported so far, indicating that the N−N bond is effectively weakened upon coordination to the $RuIr_3S_4$ cluster. By the successful preparation of the $RuIr_3S_4$ cluster ligating dinitrogen, a question emerges why this $RuIr_3S_4$ unit can bind dinitrogen but the cluster units containing other combination of metals, such as Fe−Ir_3,[9a] Mo_2−Ru_2,[9b] and Ru−Mo_3,[9c] do not form N_2 complexes. In the present study, to elucidate the nature of the bonding between the cubane-type mixed-metal clusters and N_2, we have investigated at first how N_2 is activated in **1** using density functional theory (DFT) calculations. Since the results on a model complex of **1** suggested its potential as a catalyst for N_2 reduction to NH_3, a detailed energy profile based on the Yandulov−Schrock cycle was examined by optimizing intermediates in the reaction steps as described below. We have also found that intermediates with an NNH_x (x = 1−3) ligand have a unique bent Ru−N−N linkage, which is caused by a bonding interaction between a hydrogen atom and an iridium atom in the cubane framework.[32]

2. Computational Method

All calculations were carried out with the Jaguar 6.5 program package.[33] The Cp* ligands in **1** were replaced by the Cp (η^5-C_5H_5) ligands in model complex **2** and intermediates **3**−**10** examined in this study. Optimized geometries and vibrational frequencies were computed at the B3LYP/LACVP+* level of theory.[34,35] LACVP+* represents a mixed basis set using the LanL2DZ relativistic effective core potential (RECP) for ruthenium and iridium and the standard 6−31+G(d) basis set for all other atoms. Vibrational frequencies were corrected by a scale factor of 0.96.[36] We carried out natural population analysis (NPA) calculations to obtain atomic charges and natural bond orbital (NBO) analyses to assist our understanding of the electronic structures.[37] For calculations on the energetics of the catalytic cycle, reaction enthalpies were obtained at the B3LYP/LACV3P+** level at the geometries optimized at the B3LYP/LACVP+* level. The LACV3P+** basis set uses a combination of the LanL2DZ RECP (Ru and Ir) and the 6−311+G(d,p) basis set (other atoms). The formal charge of the Cp ring is −1 and that of the sulfur atom is −2. Because the total charge of **2** is zero, the formal charges of the Ir and Ru atoms in **2** are counted to be +3 and +2, respectively; thus, both atoms having a closed-shell d^6 configuration.

On the choice of an appropriate density functional for evaluating N_2 activation on transition metal complexes, Graham and co-workers demonstrated a comparison of DFT and coupled cluster (CC) methods for a three-coordinate molybdenum complex.[38] They presented that DFT results on geometric parameters were in excellent agreement with higher-level CCSD results and that B3LYP energies qualitatively agreed with CCSD(T) ones. The B3LYP and BP86 functionals are often chosen in recent computational studies on N_2 activation on transition metal complexes relevant to Sellmann's Ru complex[15c,17–20] and Schrock's Mo complex.[26–30] For these reasons, we adopted the hybrid B3LYP functional to evaluate the degree of the N−N bond activation on the $RuIr_3S_4$ cluster and to predict the energy profile of the N_2 reduction mediated by the cluster.

To test the validity of the basis set employed in this study as well as the simplification of the Cp* ligands, we optimized the real complex **1** and the model complex **2** with the LACVP+* and LACV3P+** basis sets (see Supporting Information for details). Using the triple-ζ LACV3P+** basis set did not significantly change geometric parameters of both **1** and **2** calculated with the double-ζ LACVP+* basis set. Replacing the Cp* ligands with the Cp ligands did not influence the structure around the N_2 ligand. Therefore, to save calculation time, we decided to employ the LACVP+* basis set and adopt the simplified model complex **2**.

3. Results

3.1. Ru−N_2 Complex 2. Optimized structures of the dinitrogen complex **2** and the $RuIr_3S_4$ core **3** having a vacant coordination site on Ru are shown in Figure 2. Selected geometric parameters around the N_2 ligand in **2** are listed in Table 1, together with the corresponding experimental values of **1**. The structure of **2** reasonably reproduces the X-ray crystallographic structure of **1**, even in simplifying the Cp* ligands in **1**. Complexation does not significantly change the structure of the $RuIr_3S_4$ core, except for the bond distance

(31) Mori, H.; Seino, H.; Hidai, M.; Mizobe, Y. *Angew. Chem., Int. Ed.* **2007**, *46*, 5431.
(32) Studies to obtain the experimental evidence for the formation of NH_3 from **1** by protonation alone or coupled protonation/electronation are in progress. Unfortunately, we have still observed only the liberation of N_2 gas, followed by stoichiometric or catalytic evolution of H_2 gas, that proceeds with retention of the cluster core.
(33) *Jaguar*, version 6.5, Schrödinger, LLC: New York, 2005.
(34) (a) Becke, A. D. *Phys. Rev. A* **1988**, *38*, 3098. (b) Becke, A. D. *J. Chem. Phys.* **1993**, *98*, 5648. (c) Lee, C.; Yang., W.; Parr, R. G. *Phys. Rev. B* **1988**, *37*, 785. (d) Stephens, P. J.; Devlin, F. J.; Chabalowski, C. F.; Frisch, M. J. *J. Phys. Chem.* **1994**, *98*, 11623.
(35) (a) Ditchfield, R.; Hehre, W. J.; Pople, J. *A. J. Chem. Phys.* **1971**, *54*, 724. (b) Hehre, W. J.; Ditchfield, R.; Pople, J. A. *J. Chem. Phys.* **1972**, *56*, 2257. (c) Hariharan, P. C.; Pople, J. A. *Theor. Chim. Acta* **1973**, *28*, 213. (d) Clark, T.; Chandrasekhar, J.; Spitznagel, G. W.; Schleyer, P. v. R. *J. Comput. Chem.* **1983**, *4*, 294. (e) Francl, M. M.; Petro, W. J.; Hehre, W. J.; Binkley, J. S.; Gordon, M. S.; DeFrees, D. J.; Pople, J. A. *J. Chem. Phys.* **1982**, *77*, 3654. (f) Hay, P. J.; Wadt, W. R. *J. Chem. Phys.* **1985**, *82*, 299.
(36) Scott, A. P.; Radom, L. *J. Phys. Chem.* **1996**, *100*, 16502.
(37) Glendening, E. D. ; Badenhoop, J. K.; Reed, A. E.; Carpenter, J. E.; Bohmann, J. A.; Morales, C. M.; Weinhold, F. NBO 5.0, Theoretical Chemistry Institute, University of Wisconsin, Madison, WI, 2001; http://www.chem.wisc.edu/~nbo5.
(38) Graham, D. C.; Beran, G. J. O.; Head-Gordon, M.; Christian, G.; Stranger, R.; Yates, B. F. *J. Phys. Chem. A* **2005**, *109*, 6762.

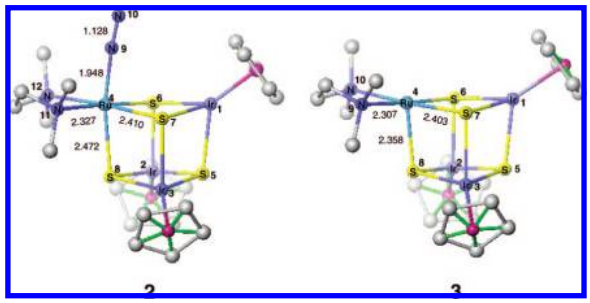

Figure 2. Optimized structures of **2** and **3** calculated at the B3LYP/LACVP+* level of theory. Hydrogen atoms are omitted for clarity. Interatomic distances (Å) and angles (deg) of **2**: Ir1−Ru4 3.587, Ir2−Ir3 3.636, Ru4−N9−N10 174.6, Ir1−Ru4−N9 83.9, Ir1−Ru4−S8 85.1, S6−Ru4−S7 82.8, N11−Ru4−N12 80.4, Ir1−Ru4−N9−N10 358.5. Interatomic distances and angles of **3**: Ir1−Ru4 3.607, Ir2−Ir3 3.622, Ir1−Ru4−S8 85.6, S6−Ru4−S7 82.7.

between the ruthenium atom and the sulfur atom located at the trans position of the N_2 ligand. The N−N bond distance and the N−N stretching frequency ν(NN) of **2** were calculated to be 1.128 Å and 2118 cm^{-1}, respectively, suggesting that the formation of the Ru−N_2 complex activates the N−N bond of dinitrogen (1.0977 Å and 2331 cm^{-1} for free dinitrogen). For a comparison between the model complex **2** and the real complex **1**, the Ru−N distance in **2** (1.948 Å) is longer than that in **1** (1.917 Å) and the value of ν(NN) of **2** is greater than that of **1** (2019 cm^{-1}). This difference implies that B3LYP-DFT calculations tend to underestimate the interaction between ruthenium and dinitrogen although the short N−N bond distance in **1** (1.06 Å) contradicts the red-shifted ν(NN) value of **1**. Tuczek and co-workers reported that DFT calculations on Fe−N_2 complexes overestimate the values of ν(NN) by 80−100 cm^{-1} compared with experimental values,[39] while calculated ν(NN) values for Mo−N_2 and W−N_2 complexes are comparable to experimental ones even in using the smaller LANL2DZ basis set.[40] An NPA calculation of **2** shows that the total atomic charges on the N_2 ligand is −0.10 (N9/N10 = −0.02/−0.08). The result that the N_2 ligand in **2** has a negative charge is important for the N−N bond activation to achieve the reduction of N_2 to NH_3 because the N_2 ligand will be attacked by an electrophile (H^+) as the first step of the reduction.

Figure 3 shows an interaction energy curve between **3** and dinitrogen as a function of the Ru−N distance calculated at the B3LYP/LACVP+* level. The binding energy was estimated to be 19 kcal/mol at an Ru−N distance of 1.95 Å. From the chemical equation **3** + N_2 → **2**, the binding energy of dinitrogen to the $RuIr_3S_4$ cluster was calculated to be 16.4 kcal/mol with a zero-point energy correction at the B3LYP/LACV3P+** level, which is in agreement with the isolation of **1**. This value is comparable to the Ru−N_2 bond energy calculated for the first Ru−N_2 complex[11] $[Ru(NH_3)_5(N_2)]^{2+}$ (21.4 kcal/mol at the B3LYP/LACV3P+** level).

3.2. Catalytic N_2 Reduction on the $RuIr_3S_4$ Cluster. Judging from the characteristics of the N_2 ligand in **2** (1.128 Å of the N−N bond distance, 2118 cm^{-1} of ν(NN) and −0.10 of the total NPA charge), the degree of N_2 activation by the $RuIr_3S_4$ cluster belongs to the "moderately activated" category in the N_2 activation scale classified by Studt and Tuczek.[12c] It is suggestive that the Mo−triamidoamine complex [Mo(N_2)(hiptN$_3$N)] is also classified into the same category. Yandulov and Schrock demonstrated that this Mo complex is capable of converting dinitrogen into ammonia with a high efficiency of ∼66% of theoretical amounts after four turnovers by choosing an appropriate pair of proton and electron sources.[22] They proposed a catalytic cycle for ammonia synthesis on the Mo complex based on the observation and isolation of a series of intermediates.[25] Here, we discuss the availability of **2** (and **1**) for catalytic ammonia synthesis from dinitrogen. The catalytic process considered here is analogous to the Yandulov−Schrock cycle,[22] which includes alternating protonation and reduction steps taking place at a single transition metal center (Figure 4). The first three protonations occur only on the terminal nitrogen atom of the N_2 ligand, resulting in diazenido (NNH), hydrazido(2−) (NNH_2), and hydrazidium (NNH_3) complexes. The N−N bond in the hydrazidium complex is cleaved to generate the first molecule of NH_3 and a nitrido (≡N) complex. The remaining nitrido complex is further protonated and reduced to form an ammine (NH_3) complex, which then releases the second molecule of NH_3.

To investigate the energy profile of the catalytic cycle by the $RuIr_3S_4$ cluster, we optimized a series of cationic/neutral complexes $[\mathbf{Ru}(NNH)]^{+/0}$ $\mathbf{4}^{+/0}$, $[\mathbf{Ru}(NNH_2)]^{+/0}$ $\mathbf{5}^{+/0}$, $[\mathbf{Ru}(NNH_3)]^{+/0}$ $\mathbf{6}^{+/0}$, $[\mathbf{Ru}(N)]^{+/0}$ $\mathbf{7}^{+/0}$, $[\mathbf{Ru}(NH)]^{+/0}$ $\mathbf{8}^{+/0}$, $[\mathbf{Ru}(NH_2)]^{+/0}$ $\mathbf{9}^{+/0}$, and $[\mathbf{Ru}(NH_3)]^{+/0}$ $\mathbf{10}^{+/0}$, where [**Ru**] is the $RuIr_3S_4$ core **3** (**Ru** = $(CpIr)_3\{Ru(tmeda)\}(\mu_3\text{-}S)_4$). For reaction enthalpy calculations, $LutH^+$ (Lut = 2,6-dimethylpyridine) and decamethylcobaltocene Cp^*_2Co were chosen as a combination of proton/electron donors, respectively. The energy profile of the protonation and reduction steps were obtained by considering the following two equations, where [X] is an intermediate.

$$[X] + LutH^+ \rightarrow [XH]^+ + Lut \quad \text{(protonation)} \quad (1)$$

$$[XH]^+ + [Cp^*_2Co] \rightarrow [XH] + [Cp^*_2Co]^+ \quad \text{(reduction)} \quad (2)$$

3.2.1. Structures of the Intermediates. Optimized structures of intermediates **3**−**10** are shown in Figures 5 and 6. Structural changes with respect to the NNH_x and NH_x moieties are summarized in Tables 1 and 2. All the lowest-energy structures of **3**−**10** have an electronic state with the lowest spin multiplicity. For example, the singlet state structure of **2** is 27.0 kcal/mol more stable than the triplet one, and the doublet structure of **7** is 19.2 kcal/mol more stable than the quartet one. It is notable that two isomeric structures owing to a bent Ru−N−N structure were found for both cationic and neutral diazenido complexes (*cis*- and *trans*-$\mathbf{4}^{+/0}$). The Ru−N−N angles are highly deviated from linearity; 149.9° (*cis*-$\mathbf{4}^+$), 156.6° (*cis*-$\mathbf{4}^0$), 145.0° (*trans*-$\mathbf{4}^+$), and 143.5° (*trans*-$\mathbf{4}^0$), but the NNH ligands remain bound to the Ru atom in an end-on manner. The cis isomer is energetically more stable than the trans isomer by 4.9 kcal/mol for $\mathbf{4}^+$ and by 2.2 kcal/mol for $\mathbf{4}^0$. The high stability of the cis isomers seems strange since it is known that the cis isomer of diazene N_2H_2 is less stable than the trans isomer for both cationic and neutral species. Hydradizo(2−) complexes $\mathbf{5}^{+/0}$ also have a bent Ru−N−N structure whose angle is close to 120°. The bent Ru−N−N structure in $\mathbf{4}^{+/0}$ and $\mathbf{5}^{+/0}$ is an intriguing finding because transition metal complexes with end-on coordinated diazenido and hydrazido(2−) ligands generally have a linear M−N−N structure (M = metal atom), which reflects a contribution from resonance structures having a

(39) Franke, O.; Wiesler, B. E.; Lehnert, N.; Tuczek, F. *Z. Anorg. Allg. Chem.* **2002**, *628*, 2395–2402.
(40) Lehnert, N.; Tuczek, F. *Inorg. Chem.* **1999**, *38*, 1659.

Table 1. Selected Bond Distances (Å) and Angles (deg) of Complexes **2**, **4**, **5**, and **6** Optimized at the B3LYP/LACVP+* Level of Theory

	2	*cis*-**4**$^+$	*trans*-**4**$^+$	*cis*-**4**^{0}	*trans*-**4**^{0}	**5**$^+$	**5**^{0}	**6**$^+$	**6**^{0}
$N_\alpha-N_\beta$	1.128 (1.06(1))[a]	1.183	1.199	1.215	1.225	1.262	1.286	1.533	1.500
$Ru-N_\alpha$	1.948 (1.917(7))[a]	1.857	1.814	1.918	1.908	1.882	1.913	1.833	1.939
$N_\beta-H$		1.084	1.033	1.051	1.044	1.041[b]	1.032[b]	1.041[b]	1.039[b]
						1.021	1.019	1.026	1.029
								1.024	1.024
$Ru-N_\alpha-N_\beta$	174.6 (172.6(9))[a]	149.9	156.6	145.0	143.5	131.1	121.7	116.4	112.4
$N_\alpha-N_\beta-H$		112.4	116.3	111.8	111.6	120.7[b]	121.8[b]	112.9[b]	112.2[b]

[a] Value for the X-ray crystallographic structure of **1**.[31] [b] Value for the hydrogen atom that is closest to Ir occupying an equatorial position of Ru.

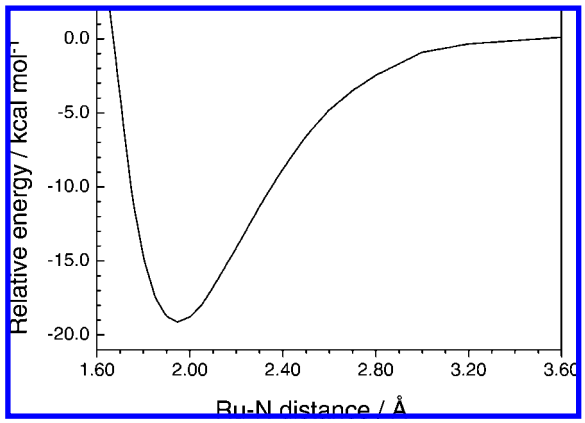

Figure 3. Interaction energy curve of **3** and dinitrogen calculated at the B3LYP/LACVP+* level of theory.

multiple-bond character in both M−N and N−N bonds.[12a,41,42] X-ray analyses for [Mo(NNH)(hiptN$_3$N)] and [Mo(NNH$_2$)(hiptN$_3$N)]$^+$ revealed that the Mo−N−N linkages are nearly linear in both the complexes (179.5° and 175.4°, respectively).[25] X-ray structural data on ruthenium complexes with the diazenido/hydrazido(2−) ligands are very scarce. To the best of our knowledge, three of aryldiazenido Ru complexes, [RuCl$_3$(*p*-N$_2$C$_6$H$_4$Me)(PPh$_3$)$_2$·X] (X = Me$_2$CO,[43a] CH$_2$Cl$_2$[43b]) and [CpRu(PPh$_3$)$_2$(N$_2$C$_6$H$_4$OMe)][BF$_4$]$_2$[43c] were reported to have a nearly linear Ru−N−N structure. Diazenido/hydrazido(2−) complexes having a bent M−N−N structure are less common, and a few X-ray crystallographic studies have been done so far only for the organo-diazenido and -hydrazido(2−) complexes.[44] Gaughan and Ibers prepared an Rh aryldiazenido complex [RhLCl(N$_2$Ph)][PF$_6$] (L = a tridentate phosphine ligand) having a Rh−N−N bond angle of 125° in the trans form.[47] Colin and co-workers reported that [Mo(N$_2$Ph)$_2$(TTP)] (TTP = *meso*-tetratolylporphyrin dianion) has two trans-bent Mo−N−N linkages (Mo−N−*N* = 149.1°).[48] For hydrazido(2−) complexes, Dilworth and co-workers showed that [ReBr$_2$(N$_2$Ph)(N$_2$HPh)(PPh$_3$)$_2$] has a hydrazido(2−) ligand with a large angular distortion (Re−N−N= 131.2°).[49] Coia and co-workers reported that an Os complex [Os(NNEt$_2$)(tpy)(bpy)][PF$_6$]$_2$ has an Os−N−N bond angle of 137°.[50] In the following section, we turn our attention to how the NNH$_x$ ligand is bonded to the RuIr$_3$S$_4$ core.

Here, we distinguish two nitrogen atoms of the N_2 ligand as N_α and N_β, where N_α is the nitrogen atom directly bound to the Ru atom and N_β is the remote one. An increase in the number of hydrogen atoms on N_β elongates the $N_\alpha-N_\beta$ distance except for **6**^{0}; 1.128 Å (**2**) → 1.183 Å (**4**$^+$) → 1.215 Å (**4**^{0}) → 1.262 Å (**5**$^+$) → 1.286 Å (**5**^{0}) → 1.533 Å (**6**$^+$) → 1.500 Å (**6**^{0}). The gradual increase in the $N_\alpha-N_\beta$ distance indicates that the successive protonations weaken the N−N bond. On the other hand, the Ru−N_α distance in **2**−**6** does not depend on the number of hydrogen atoms on N_β; 1.948 Å (**2**) → 1.857 Å (**4**$^+$) → 1.918 Å (**4**^{0}) → 1.882 Å (**5**$^+$) → 1.913 Å (**5**^{0}) → 1.833 Å (**6**$^+$) → 1.939 Å (**6**^{0}). The neutral complexes tend to have a longer Ru−N_α distance than the corresponding cationic ones. The Ru−N_α distances in **2**−**6** imply that the hydrogenation of dinitrogen would not significantly change the strength of the interaction between the Ru atom and N_2. The correlation between the N−N and Ru−N bond distances is quite different from the case of Schrock's Mo complex.[25] In the X-ray crystallographic structures of [**Mo**(N$_2$)], [**Mo**(NNH)], and [**Mo**(NNH$_2$)]$^+$ (**Mo** = Mo(hiptN$_3$N)), the $N_\alpha-N_\beta$ distances are 1.061, 1.302, and 1.304 Å, respectively, while the Mo−N_α bond distances are 1.963, 1.780, and 1.743 Å. The hydrogenation of the N_2 ligand apparently strengthens the Mo−N bond.

For complexes **7**-**10**, [**Ru**(NH$_x$)] (x = 0−3), the correlation between the Ru−N_α distance and the number of hydrogen atoms on N_α is reasonable; 1.693 Å (**7**) → 1.798 Å (**8**$^+$) → 1.829 Å (**8**^{0}) → 1.922 Å (**9**$^+$) → 2.006 Å (**9**^{0}) → 2.269 Å (**10**$^+$) → 2.270 Å (**10**^{0}). The change in the Ru−N_α distance indicates that the Ru−N bond in [**Ru**(NH$_x$)] is weakened by the successive hydrogenations, which is similar to the case of Schrock's Mo complexes.[25]

(41) Sutton, D. *Chem. Rev.* **1993**, *93*, 995.
(42) (a) Masumori, T.; Seino, H.; Mizobe, Y.; Hidai, M. *Inorg. Chem.* **2000**, *39*, 5002. (b) Davis, S. C.; Hughes, D. L.; Konkol, M.; Richards, R. L.; Sanders, J. R.; Sobota, P. *J. Chem. Soc., Dalton Trans.* **2002**, 2811. (c) Janas, Z.; Jerzykiewicz, L. B.; Richards, R. L.; Sobota, P. *Inorg. Chim. Acta* **2003**, *350*, 379. (d) Horn, K. H.; Böres, N.; Lehnert, N.; Mersmann, K.; Näther, C.; Peters, G.; Tuczek, F. *Inorg. Chem.* **2005**, *44*, 3016. (e) Odom, A. L.; Banerjee, S. *Organometallics* **2006**, *25*, 3099.
(43) (a) McArdle, J. V.; Schultz, A. J.; Corden, B. J.; Eisenberg, R. *Inorg. Chem.* **1973**, *12*, 1676. (b) Haymore, B. L.; Ibers, J. A. *Inorg. Chem.* **1975**, *14*, 3060. (c) Fan, L.; Einstein, F. W. B.; Sutton, D. *Organometallics* **2000**, *19*, 684.
(44) As for the exceptional structures of the parent NNH$_2$ ligand, the bent M−N−N linkage has been proposed for the Zr(IV) complex by the DFT study,[45] while η^2-coordination at two N atoms has been suggested spectroscopically for the W(VI) complexes.[46]
(45) Herrmann, H.; Fillol, J. L.; Wadepohl, H.; Gade, L. H. *Angew. Chem., Int. Ed.* **2007**, *46*, 8426.
(46) (a) Glassman, T. E.; Vale, M. G.; Schrock, R. R. *J. Am. Chem. Soc.* **1992**, *114*, 8098. (b) Wagenknecht, P. S.; Norton, J. R. *J. Am. Chem. Soc.* **1995**, *117*, 1841.
(47) Gaughan, A. P.; Haymore, B. L.; Ibers, J. A.; Myers, W. H.; Nappoer, T. E., Jr.; Meek, D. W. *J. Am. Chem. Soc.* **1973**, *95*, 6859.
(48) Colin, J.; Butler, G.; Weiss, R. *Inorg. Chem.* **1980**, *19*, 3828.
(49) Dilworth, J. R.; Harrison, S. A.; Walton, D. R. M.; Schweda, E. *Inorg. Chem.* **1985**, *24*, 2594.
(50) Coia, G. M.; Devenney, M.; White, P. S.; Meyer, T. J. *Inorg. Chem.* **1997**, *36*, 2341.

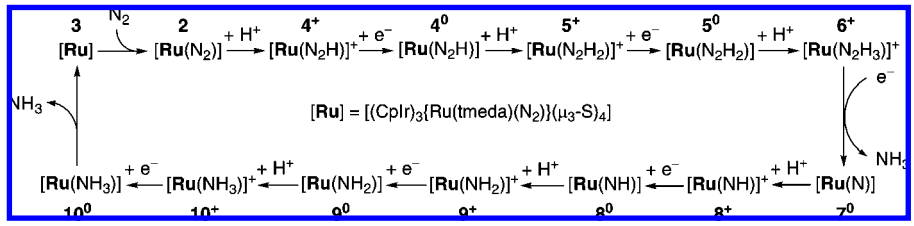

Figure 4. Catalytic cycle of the conversion of dinitrogen into ammonia in the cubane-type $RuIr_3S_4$ cluster system examined in this study. Numbering of the intermediates is described in the text.

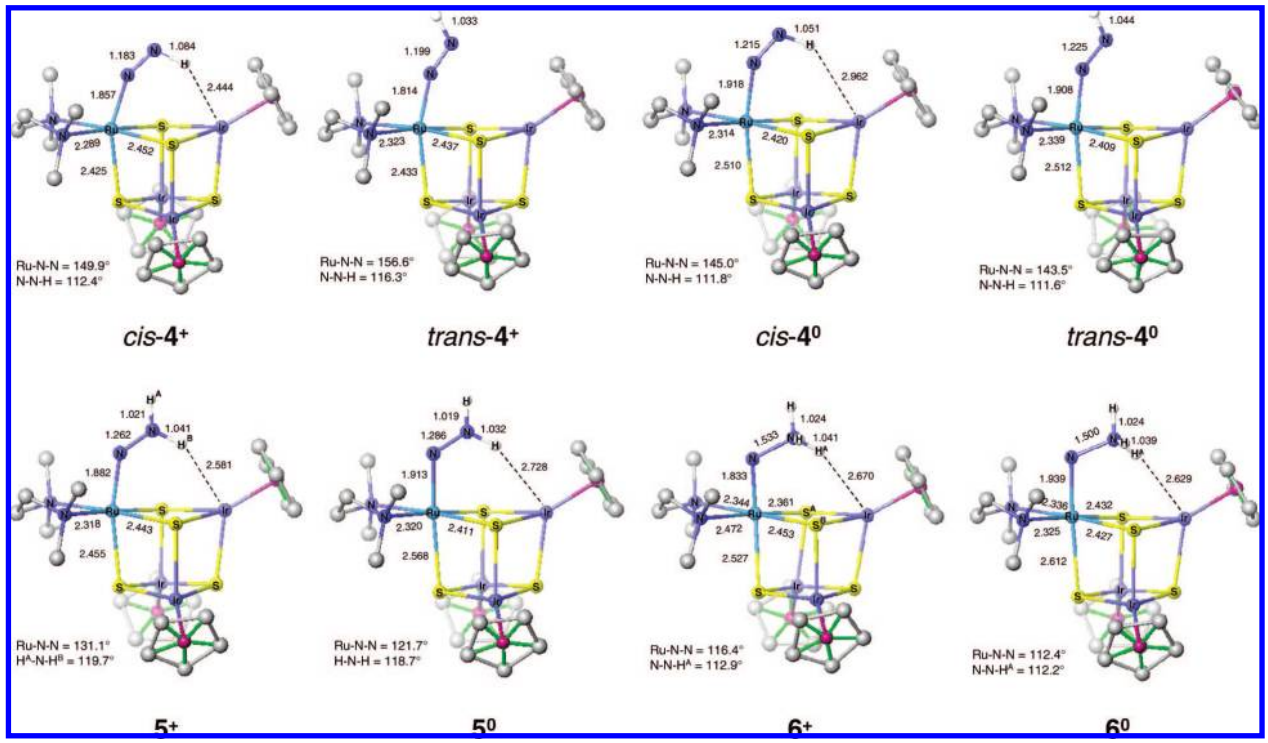

Figure 5. Optimized structures of $\mathbf{4}^{+/0}$–$\mathbf{6}^{+/0}$ at the B3LYP/LACVP+* level of theory. Hydrogen atoms are omitted for clarity.

3.2.2. Energy Profile of the Catalytic Cycle. A calculated energy profile for the catalytic conversion of N_2 into NH_3 by [**Ru**] **3** is shown in Figure 7. Calculated reaction enthalpies include the zero-point energy correction although solvent and thermal effects are not considered. At the first stage of N_2 reduction, the starting complex **3** binds dinitrogen to form [**Ru**(N_2)] **2**. As described in this manuscript, the binding energy of dinitrogen to **2** was calculated to be 16.4 kcal/mol. The value of ΔH_0 for the first protonation of **2** to give $\mathbf{4}^+$ is as large as 17.8 kcal/mol, which is the most endothermic in all the steps of the catalytic cycle. The following reaction steps to yield the neutral hydrazido(2−) complex $\mathbf{5}^{\mathbf{0}}$ are found to be exothermic. The next two steps, in which $\mathbf{5}^{\mathbf{0}}$ is protonated and reduced to $\mathbf{6}^{\mathbf{0}}$, are nearly thermoneutral. These results are very similar to the result on Schrock's Mo complex reported by Studt and Tuczek.[27] For the N−N bond cleavage to generate the first molecule of NH_3, we considered two reaction routes. One is that $\mathbf{6}^+$ is reduced to $\mathbf{6}^{\mathbf{0}}$, followed by the formation of the neutral nitrido complex $\mathbf{7}^{\mathbf{0}}$ and NH_3. The other is that $\mathbf{6}^+$ is split into $\mathbf{7}^+$ and NH_3 in advance, and then $\mathbf{7}^+$ is reduced to give $\mathbf{7}^{\mathbf{0}}$. In the former route, the reduction of $\mathbf{6}^+$ is thermoneutral and the formation of $\mathbf{7}^{\mathbf{0}}$ and NH_3 is exothermic by 19.0 kcal/mol. In the latter route, both the N−N bond cleavage of $\mathbf{6}^+$ and the reduction of $\mathbf{7}^+$ are exothermic by 13.9 and 5.2 kcal/mol, respectively. The enthalpies calculated for the N−N bond cleavage indicate that both reaction routes are reasonable for the $RuIr_3S_4$ cluster system. It is notable that the neutral hydrazidium complex $\mathbf{6}^{\mathbf{0}}$ was optimized as a stable intermediate. For Schrock's Mo complex, computational studies revealed that the reduction of the cationic Mo−NNH_3 complex immediately breaks the N−N bond to generate the first NH_3 molecule.[26,27,29,30] With DFT-based molecular dynamics simulations on the reduced form of the cationic Mo−NNH_3 complex at 0 K, Magistrato and co-workers presented that the release of NH_3 from the cationic Mo−NNH_3 complex occurred with no energy barrier.[30] Calculated enthalpies for the formation of [**Ru**(NH_x)] indicate that the successive protonations of N_α to generate the second molecule of NH_3 are highly exothermic; −31.0 kcal/mol for $\mathbf{7}^{\mathbf{0}} \rightarrow \mathbf{8}^+$, −51.9 kcal/mol for $\mathbf{8}^{\mathbf{0}} \rightarrow \mathbf{9}^+$, and −45.6 kcal/mol for $\mathbf{9}^{\mathbf{0}} \rightarrow \mathbf{10}^+$. Finally, the ammine complex $\mathbf{10}^{\mathbf{0}}$ requires 11.0 kcal/mol to afford [**Ru**] **3** and the second molecule of NH_3. Because the binding energy of N_2 to **3** is as large as 16.4 kcal/mol, the substitution of NH_3 by N_2 is 5.4 kcal/mol exothermic.

The overall enthalpy change calculated for this cycle (from the left to the right in Figure 7) is highly negative (−193.4 kcal/mol), corresponding to the ΔH_0 value obtained for the following reaction,

$$N_2 + 6LutH^+ + 6Cp^*_2Co \rightarrow 2NH_3 + 6Lut + 6Cp^*_2Co^+ \quad (3)$$

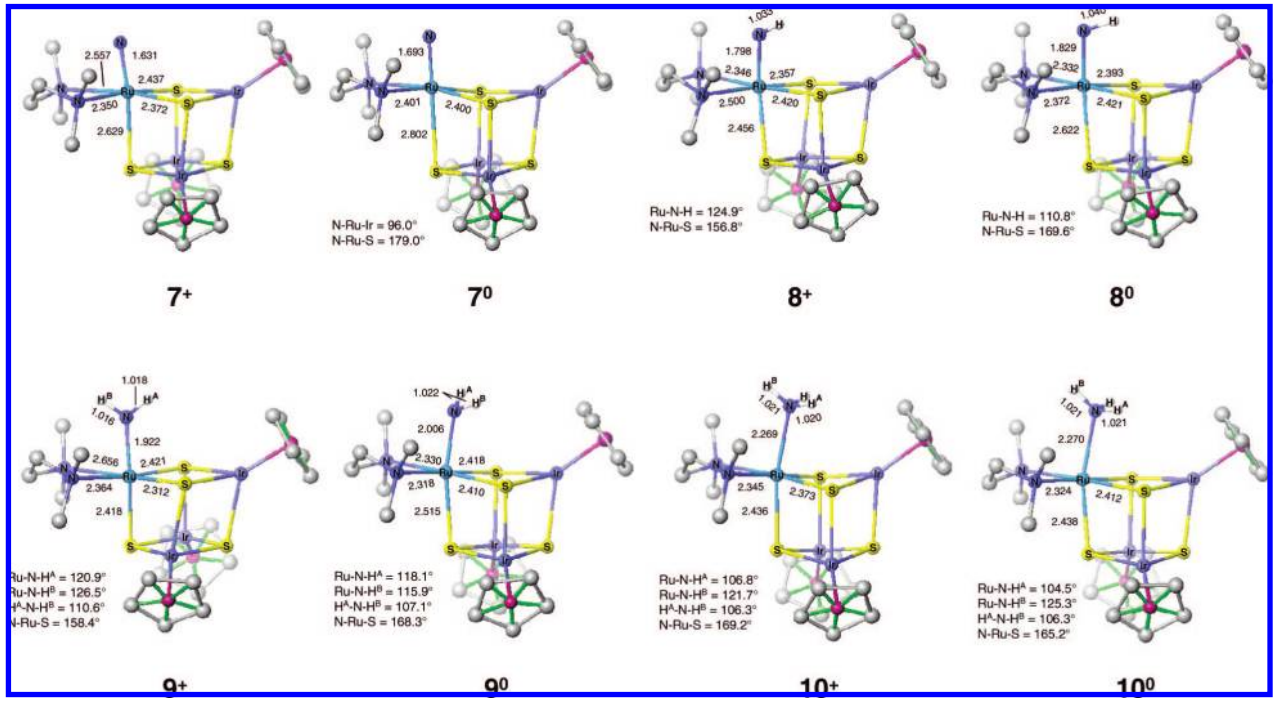

Figure 6. Optimized structures of $\mathbf{7}^{+/0}-\mathbf{10}^{+/0}$ at the B3LYP/LACVP+* level of theory. Hydrogen atoms are omitted for clarity.

Table 2. Selected Bond Distances (Å) and Angles (deg) of Complexes **7**−**10** Optimized at the B3LYP/LACVP+* Level of Theory

	$\mathbf{7}^{+}$	$\mathbf{7}^{0}$	$\mathbf{8}^{+}$	$\mathbf{8}^{0}$	$\mathbf{9}^{+}$	$\mathbf{9}^{0}$	$\mathbf{10}^{+}$	$\mathbf{10}^{0}$
Ru−N_α	1.631	1.693	1.798	1.829	1.922	2.006	2.269	2.270
N_α−H[a]			1.033	1.040	1.017	1.022	1.020	1.021
Ru−N_α−H^A [b]			124.9	110.8	120.9	118.1	106.8	104.5
Ru−N_α−H^B [b]					126.5	115.9	121.7	125.3
H^A−N_α−H^B [b]					110.6	107.1	106.3	106.3

[a] Average value of all hydrogen atoms. [b] For labeling on the hydrogen atoms, see Figure 6.

The energy profile calculated for the $RuIr_3S_4$ cluster resembles that for the model of Schrock's complex reported by Studt and Tuczek[27] in three points: (1) the N_2 binding energy (16.4 kcal/mol vs 14.2 kcal/mol), (2) the enthalpy change for the first protonation (17.8 kcal/mol vs 21.5 kcal/mol), which is the most endothermic in both the cycles, and (3) the enthalpy change for the NH_3/N_2 exchange reaction (5.4 kcal/mol vs 5.4 kcal/mol).[51] However, as pointed out by Reiher and co-workers, the two energy profiles must be compared with care because the model complex adopted by Studt and Tuczek is oversimplified and the presence of bulky substituents surrounding the Mo atom is crucial for discussing the energetics.[28,29] A computational study on the real Schrock's complex without any simplification revealed that the enthalpy changes for the N_2 binding and the NH_3/N_2 exchange reaction are exothermic at the BP86/RI/TZVP level of theory by 37.5 and 9.7 kcal/mol, respectively,[29] which are much greater than the values reported by Studt and Tuczek. Using another model of Schrock's complex, in which the hipt substituents are replaced by phenyl groups, Cao and co-workers reported that the N_2 binding energy was calculated to be 32 kcal/mol (PW91 functional) and 16 kcal/mol (BLYP functional), while the NH_3/N_2 exchange reaction is endothermic by 4 kcal/mol (BLYP).[26] With the same model as Cao et al. employed, Magistrato and co-workers presented that the energy profile of the Yandulov−Schrock cycle is quite different from the results reported by Studt and Tuczek.[30] The calculated energy profile involves several endothermic reaction steps with small enthalpy changes (~8 kcal/mol). In their calculation, the N_2 binding and the NH_3/N_2 exchange reaction are exothermic by 29 and 8 kcal/mol, respectively, which are close to the values reported by Reiher et al. In conclusion, the energy profile calculated for the catalytic cycle indicates that the $RuIr_3S_4$ cluster system has good potential as a catalyst for N_2 reduction, if a pair of proton/electron donors is appropriately chosen.

4. Discussion

In this section, we would like to discuss the bonding nature of a series of complexes consisting of the $RuIr_3S_4$ cluster and an NNH_x ($x = 0-3$) ligand based on geometric structures and results of the NBO analysis. To clarify the influence of the cuboidal metal sulfido framework upon the bonding between the Ru atom and the NNH_x ligand, we have investigated the geometric and electronic structures of $[Ru(NH_3)_5(N_2)]^{2+}$ **11** and its hydrogenated derivatives $[\mathbf{Ru'}(NNH_x)]^{+/0}$ $\mathbf{12}^{+/0}-\mathbf{14}^{+/0}$ ($[\mathbf{Ru'}]^{+/0} = [Ru(NH_3)_5]^{3+/2+}$; $x = 1-3$) at the B3LYP/LACVP+* level of theory. $[\mathbf{Ru'}(N_2)]$ **11** is one of the simplest transition metal−dinitrogen complexes although the N_2 ligand in **11** cannot be protonated.[52] Selected geometric parameters around the Ru−NNH_X moiety of **2**, **4**−**6**, and **11**−**14** are listed in Table 3. The Ru−N_α−N_β angle as well as the bond distances is a useful parameter for judging a multiple-bond character of the N−N bond because the Ru−N_α−N_β angles depend on the degree of s-p hybridization of N_α and N_β.

4.1. Dinitrogen Complexes 2 and 11. As seen in Table 3, the geometric parameters of the Ru−N_2 moiety of $[\mathbf{Ru}(N_2)]$ **2** are very close to those of $[\mathbf{Ru'}(N_2)]$ **11**. However, the NBO analysis

(51) This value is the Gibbs free energy change at 298 K (ΔG_{298}) and solvent effects are taken into account (in heptane). See ref 27.

(52) Allen, A. D.; Harris, R. O.; Loescher, B. R.; Stevens, J. R.; Whiteley, R. N. *Chem. Rev.* **1973**, *73*, 11.

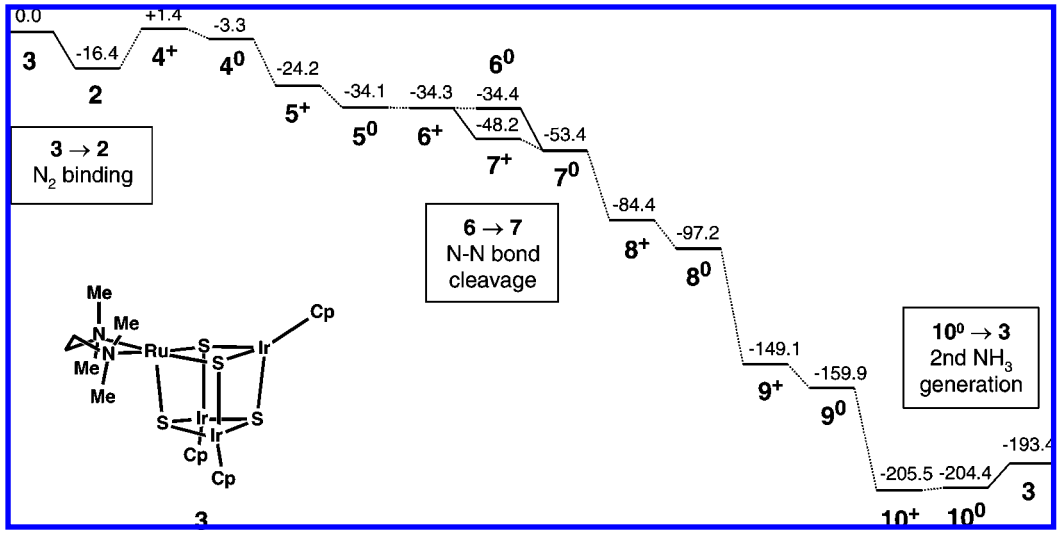

Figure 7. Energy profile for the catalytic ammonia synthesis in the $RuIr_3S_4$ cluster system calculated at the B3LYP/LACV3P+** level of theory (units in kcal/mol). Details on the catalytic cycle are shown in Figure 4. Dotted lines connecting intermediates represent protonation or one-electron reduction steps.

Table 3. Selected Bond Distances (Å) and Angles (deg) of [**Ru′**(NNH$_x$)] **11-14** (**Ru′** = $[Ru(NH_3)_5]^{2+}$; $x = 0-3$), $\mathbf{5}^{2+}$, and $\mathbf{13}^{2+}$ Optimized at the B3LYP/LACVP+* Level of Theory

complex	**11**	$\mathbf{12}^{+}$	$\mathbf{12}^{0}$	$\mathbf{13}^{+}$	$\mathbf{13}^{0}$	$\mathbf{14}^{+}$	$\mathbf{14}^{0}$	$\mathbf{5}^{2+}$	$\mathbf{13}^{2+}$
x	0	1	1	2	2	3	3		2
$N_\alpha-N_\beta$	1.115	1.134	1.202	1.236	1.264	1.513	1.507	1.251	1.229
$Ru-N_\alpha$	1.997	1.867	1.938	1.877	1.927	1.806	1.934	1.841	1.796
$N_\beta-H$		1.035	1.040	1.036 [a]	1.028[a]	1.034[a]	1.029[a]	1.061[b] 1.023	1.052[a]
$Ru-N_\alpha-N_\beta$	179.9	177.7	138.1	160.7	128.4	128.6	123.6	137.4	179.1
$N_\alpha-N_\beta-H$		167.1	117.3	122.0[a]	122.0[a]	111.0[a]	111.5[a]	119.5[a]	121.9[a]

[a] Average value for all hydrogen atoms. [b] Value for the hydrogen atom which is closest to Ir occupying an equatorial position of Ru.

revealed a significant difference in their electronic structures. The NPA charges on N_α and N_β in **2** calculated to be −0.02 and −0.08, respectively, indicate that the $RuIr_3S_4$ core provides a small amount of electrons to the π^* orbital of the dinitrogen and reductively activates the dinitrogen. On the other hand, the dinitrogen bound to **11** has a total charge of +0.09 (−0.05 on N_α and +0.14 on N_β). The central ruthenium atom of **11** withdraws a small amount of electrons from the bonding orbitals of the N_2 ligand, resulting in a long N−N distance and a red-shifted ν(NN) relative to free dinitrogen. The NBO analysis assigned 1.72 (**2**) and 1.66 (**11**) electrons to lone pair electrons on N_β, respectively, while 0.36 (**2**) and 0.18 (**11**) electrons are allocated for the N−N π^* orbital. In the coordinate bonding between Ru and N_2, the σ donation to metal (Ru dσ ←:N≡N) is greater in **11**, while the π-back-donation to dinitrogen (Ru dπ → N−N π^*) is greater in **2**. The strong electron-donating ability of the three sulfido ligands in **2** would contribute to the difference in the Ru−N_2 bonding between **2** and **11**.[31] We should stress again that a negatively charged N_2 ligand is essential for the catalytic N_2 reduction achieved by the Yandulov−Schrock cycle because the N_2 ligand must be attacked by an electrophile (H^+) to form a diazenido complex. Actually, the protonation of **11** to give $\mathbf{12}^{+}$ is highly endothermic (ΔH_0 = 228 kcal/mol; LutH^+ as a proton source).

4.2. Diazenido Complexes $\mathbf{4}^{+/0}$ and $\mathbf{12}^{+/0}$. The diazenido complex **4** has two isomeric structures, *cis*- and *trans*-$\mathbf{4}^{+/0}$. There are two questions to be answered with respect to the structure of $\mathbf{4}^{+/0}$. The first is the reason for the highly bent Ru−N−N structure ($Ru-N_\alpha-N_\beta$ = 149.9° in *cis*-$\mathbf{4}^{+}$), and the second is the reason that the cis isomer is energetically more favorable than the trans isomer. For all of the metal−aryldiazenido complexes with a bent M−N−N structure reported, the metal atom and the ArN_2 ligand (Ar = aryl group) are connected to each other in the trans form.[52,53] In the cis isomers, the hydrogen atom of the N_2H ligand locates close to the iridium atom located at an equatorial position of the ruthenium center. The $N_\beta-H$ distance in *cis*-$\mathbf{4}^{+}$ was calculated to be 1.084 Å, which is very long compared with the $N_\beta-H$ distance in *trans*-$\mathbf{4}^{+}$ (1.033 Å). The long $N_\beta-H$ distance in *cis*-$\mathbf{4}^{+}$ is associated with the low $N_\beta-H$ stretching frequency (2404 cm^{-1}), which is extremely red-shifted relative to the value for *trans*-$\mathbf{4}^{+}$ (3193 cm^{-1}). On the other hand, the short Ir−H distance (2.444 Å) implies that the hydrogen atom is attracted by the nearest iridium atom.

Figure 8 depicts the MOs of *cis*- and *trans*-$\mathbf{4}^{+}$ contributing to the π-back-donation in the Ru−N bond. Only in the MO of *cis*-$\mathbf{4}^{+}$, another bonding interaction can be found between the d orbital of Ir and the s orbital of H. The presence of the Ir−H interaction in *cis*-$\mathbf{4}^{+}$ makes it possible to answer the two questions on the structure of *cis*-$\mathbf{4}^{+}$ because the crystalline structures of Ru−N_2Ar complexes previously reported[47] as well as the optimized structure of [**Ru′**$(N_2H)]^+$ $\mathbf{12}^{+}$ adopt a linear or slightly trans-bent Ru−N−N structure (171.2−175.4°). The Ru−N distance in *cis*-$\mathbf{4}^{+}$ (1.857 Å) is longer than that in *trans*-$\mathbf{4}^{+}$ (1.814 Å), while the N−N distance in *cis*-$\mathbf{4}^{+}$ (1.183 Å) is shorter than that in *trans*-$\mathbf{4}^{+}$ (1.199 Å). The Ru−N−N angle in *trans*-$\mathbf{4}^{+}$ (156.6°) is closer to linearity than that in *cis*-$\mathbf{4}^{+}$ (149.9°). The geometric parameters of the Ru−N−N−H moiety

(53) Bowden, W. L.; Little, W. F.; Meyer, T. J. *J. Am. Chem. Soc.* **1973**, *95*, 5084.

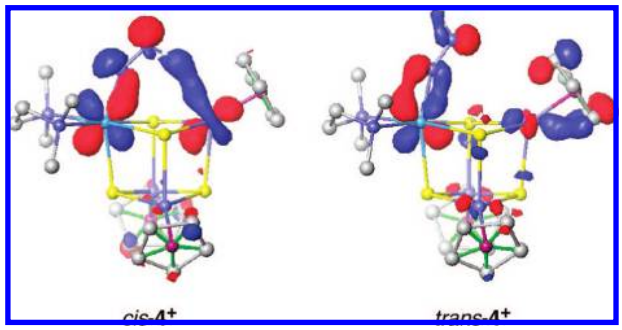

Figure 8. Spatial distributions of MO144 of *cis*- and *trans*-$\mathbf{4}^+$. A bonding interaction between Ir and H is found only in *cis*-$\mathbf{4}^+$. Hydrogen atoms are omitted for clarity.

indicate that the bonding between the Ru atom and the N_2H ligand is stronger in *trans*-$\mathbf{4}^+$. This is because both the σ and π interactions between the Ru atom and the N_2H ligand are more intensified when the Ru−N−N structure is closer to linearity. In the diazenido complexes of the $RuIr_3S_4$ cluster, the stabilization caused by the Ir−H interaction overcomes not only the stronger Ru−N_2 interaction by adopting a linear Ru−N−N linkage but also the destabilization by adopting the *cis*-Ru−N−N−H geometry.

Next we consider a contribution of sulfur atoms consisting of the cubane framework to the stabilization of the *cis*-Ru−N−N−H geometry via N−H−S hydrogen bridges. For mono- and dinuclear metal−thiolate complexes ligating N_2H_2 (metal = Ru, Fe), Reiher and co-workers reported that hydrogen bonds between the sulfur ligands and the hydrogen atoms of N_2H_2 play an essential role in stabilizing the reactive N_2H_2 species and they evaluated the energetic contribution of the N−H−S hydrogen bonds to the stabilization by adopting the *trans*-H−N−N−H structure.[17–20] In *cis*-$\mathbf{4}^+$, the N_2H ligand is located in the middle of the two nearest sulfur atoms and the H−S distances are calculated to be 2.920 and 2.914 Å, which are too long to find hydrogen bonds on the basis of a distance criterion.[17] Thus, the Ir−H interaction would predominantly govern the stability of the *cis*-Ru−N−N−H structure in the diazenido complexes of the $RuIr_3S_4$ cluster.

The *cis*-Ru−N−N−H geometry in the diazenido complex might provide an advantage from the viewpoint of reaction dynamics for the second protonation. As shown in Figure 9, N_α of the N_2H ligand is sterically hindered by the bulky substituents on the Ru and Ir atoms. Since the hydrogen atom bound to N_β is fixed by the iridium atom in the cis isomer, the lobe of the lone pair electrons of N_β points toward the space above the cluster. As a result, the lone pair electrons of N_β in *cis*-$\mathbf{4}^\mathbf{0}$ could be attacked by a proton to form the hydrazido(2−) complex $\mathbf{5}^+$ easier than *trans*-$\mathbf{4}^\mathbf{0}$. The activation energy for the protonation of *cis*-$\mathbf{4}^\mathbf{0}$ would be smaller than that for the protonation of *trans*-$\mathbf{4}^\mathbf{0}$ because the structural change from *cis*-$\mathbf{4}^\mathbf{0}$ to $\mathbf{5}^+$ is not significant, as seen in Figure 5. In summary, the presence of the iridium atom located at an equatorial position of the ruthenium atom (or the cuboidal $RuIr_3S_4$ framework itself) plays an important role not only in determining the coordination mode of the N_2H ligand but also in the energetics of the catalytic cycle.

Finally, we discuss the electronic structure of *cis*-$\mathbf{4}^{+/0}$ and compare it with that of $[\mathbf{Ru'}(N_2H)]^{+/0}$ $\mathbf{12}^{+/0}$. Since extensive synthetic studies in the 1970s, it is known that the ArN_2 ligand in metal−aryldiazenido complexes shows a duality in the metal−nitrogen bonding (Chart 1).[41,47,53] When the M−N_α−N_β angle in an M−N_2Ar complex is close to 180°, one can consider the contribution of structure **Ib**, which gives a double-bond character to both the M−N_α and N_α−N_β bonds. In this case, the ArN_2 ligand behaves as ArN_2^+. If the M−N_α−N_β bond angle is close to 120°, it is reasonable to consider that N_α adopts sp^2 hybridization and the ArN_2 ligand is described as ArN_2^- (structure **II**). For $\mathbf{4a}^+$, the sum of NPA charges on the N_2H ligand is nearly zero (+0.07) and the Ru−N_α−N_β angle is 149.9°, both of which are just between the ideal values for ArN_2^+ and ArN_2^-. Considering the long Ru−N_α distance (1.857 Å) relative to that in the imido complex $[\mathbf{Ru}(NH)]^+$ $\mathbf{8}^+$ (1.798 Å), *cis*-$\mathbf{4}^+$ should have a single Ru−N bond rather than a double bond. From these results, the electronic structure of *cis*-$\mathbf{4}^+$ is best described as [**Ru**(III)(N═NH)]. For $\mathbf{12}^+$, the positive charge on the N_2H ligand as well as the long Ru−N_α distance (1.867 Å) indicates that the electronic structure should be viewed as $[\mathbf{Ru'}(II)\leftarrow(:N{\equiv}NH)^+]$. The neutral complex *cis*-$\mathbf{4}^\mathbf{0}$ has a geometry close to *cis*-$\mathbf{4}^+$ except for the longer Ru−N_α distance (1.918 Å). The N_2H ligand in *cis*-$\mathbf{4}^\mathbf{0}$ has a total NPA charge of −0.16 and the Ru−N_α−N_β angle is 145.0°. The natural spin density calculated for *cis*-$\mathbf{4}^\mathbf{0}$ is delocalized on the Ru atom and N_α. After all, the electronic structure of *cis*-$\mathbf{4}^\mathbf{0}$ should be described as $[\mathbf{Ru}(III)(N{=}NH)^-]$ or [**Ru**(II)(N═NH)]. For $\mathbf{12}^\mathbf{0}$, the geometric parameters of the N_2H ligand are close to those in *cis*-$\mathbf{4}^\mathbf{0}$ and the total charge on the N_2H ligand is nearly zero (+0.06). The electronic structure of $\mathbf{12}^\mathbf{0}$ should be thus described as $[\mathbf{Ru'}(II)(N{=}NH)]$.

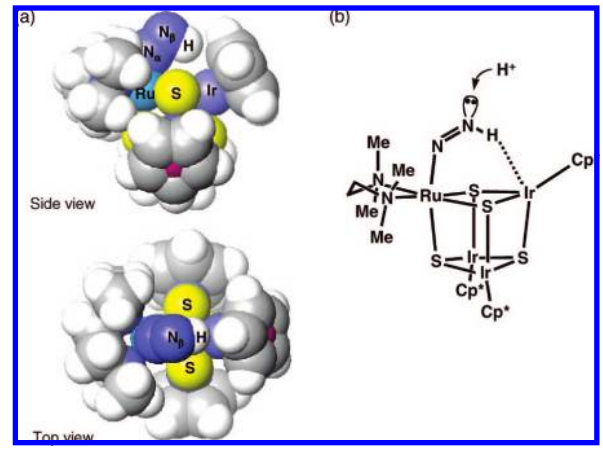

Figure 9. (a) Space-filling model views and (b) a schematic drawing of *cis*-$\mathbf{4}^\mathbf{0}$. The Ru center and N_α are protected by bulky substituents and the hydrogen atom bound to N_β is fixed by Ir through the Ir−H interaction. The direction of lone pair electrons on N_β is emphasized in part b.

Chart 1. Duality in Coordination Modes of a Diazenido Ligand N_2R (R = H, aryl group) to Metal

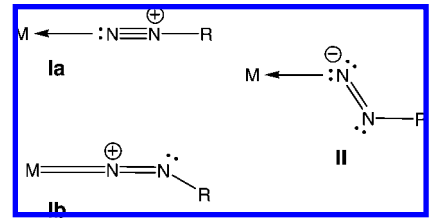

4.3. Hydrazido(2−) Complexes $\mathbf{5}^{+/0}$ and $\mathbf{13}^{+/0}$. The hydrazido(2−) complexes $\mathbf{5}^{+/0}$ have a bent Ru−N−N structure, while transition metal−hydrazido(2−) complexes generally have a nearly linear Ru−N−N structure.[12a] The reason for the bent Ru−N−N structure in $\mathbf{5}^{+/0}$ and $\mathbf{13}^{+/0}$ is explained by looking at their HOMOs. As depicted in Figure 10, the HOMO is

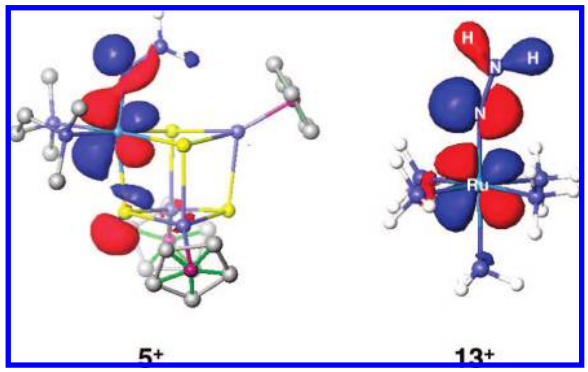

Figure 10. Spatial distributions of the singly occupied MOs of $\mathbf{5}^+$ and $\mathbf{13}^+$. Hydrogen atoms in $\mathbf{5}^+$ are omitted for clarity.

antibonding between the Ru dπ and N_αp orbitals in the Ru−NNH_2 plane. The Ru−N−N moiety in $\mathbf{5}^{+/0}$ and $\mathbf{13}^{+/0}$ adopts a bent linkage to reduce the antibonding character between the Ru atom and N_α. However, the large difference in the Ru−N_α−N_β angle between $\mathbf{5}^+$ (131.1°) and $\mathbf{13}^+$ (160.7°) reminds us of the presence of the Ir−H interaction in $\mathbf{5}^+$, similar to the diazenido complex *cis*-$\mathbf{4}^+$. So, we optimized the structure of doubly cationic complexes $\mathbf{5}^{2+}$ and $\mathbf{13}^{2+}$ to examine the structural changes of $\mathbf{5}^+$ and $\mathbf{13}^+$ by removing an unpaired electron. In $\mathbf{5}^{2+}$ and $\mathbf{13}^{2+}$, there is no electron occupying the antibonding MO that causes the bending of the Ru−N−N bonding. Geometric parameters of the Ru−NNH_2 moiety of $\mathbf{5}^{2+}$ and $\mathbf{13}^{2+}$ are listed in Table 3. As expected, removing one electron from the SOMO of $\mathbf{13}^+$ makes the Ru−N−N linkage in $\mathbf{13}^{2+}$ linear (179.1°), while $\mathbf{5}^{2+}$ still retains a bent Ru−N−N linkage of 137.4°. The N_β−H^B distance in $\mathbf{5}^{2+}$ (1.061 Å) is longer than that in $\mathbf{5}^+$ (1.041 Å) and the Ir−H^B distance (2.395 Å) in $\mathbf{5}^{2+}$ is much shorter than that in $\mathbf{5}^+$ (2.581 Å). These parameters indicate that removing one electron from $\mathbf{5}^+$ would strengthen the electrostatic attraction between the Ir atom and H^B. From the comparison between $\mathbf{5}^+$ and $\mathbf{13}^+$, the presence of the Ir atom plays a key role in determining the geometry of the hydrazido(2−) complex of the $RuIr_3S_4$ cluster. On the other hand, similar to the diazenido complex *cis*-$\mathbf{4}^+$, the N−H−S hydrogen bonds would not be essential for the bent Ru−N−N structure of $\mathbf{5}^+$ because the NNH_2 ligand is located in the middle of the two nearest sulfur atoms and the H−S distances (2.850 and 2.878 Å) are too long on the basis of a distance criterion of hydrogen bonds.

Let us next discuss how the electronic structures of $\mathbf{5}^{+/0}$ and $\mathbf{13}^{+/0}$ are described. The hydrazido(2−) complexes $\mathbf{5}^{+/0}$ have long Ru−N_α bond distances (1.882 Å for $\mathbf{5}^+$ and 1.913 Å for $\mathbf{5}^0$), which are comparable to the values for $\mathbf{4a}^{+/0}$. The small Ru−N_α−N_β angles of $\mathbf{5}^+$ (131.1°) and $\mathbf{5}^0$ (121.7°) as well as lone pair electrons on N_α assigned by the NBO analysis indicate a single-bond character of the Ru−N bonding in $\mathbf{5}^{+/0}$. The N_α−N_β distances of $\mathbf{5}^+$ (1.262 Å) and $\mathbf{5}^0$ (1.286 Å) are close to the N−N distance in diazene HN═NH (1.25 Å). The N_α−N_β distances and the planarity of the NNH_2 ligand (H−N−N−H = 178.9°) in $\mathbf{5}^{+/0}$ strongly suggest that the N−N bond should have a double-bond character and both N_α and N_β have the sp^2 electron configuration. The total NPA charge on the NNH_2 ligand in $\mathbf{5}^+$ is positive (+0.17; −0.16 for N_α and +0.33 for $N_\beta H_2$), while that in $\mathbf{5}^0$ is nearly zero (−0.03; −0.26 for N_α and +0.23 for $N_\beta H_2$). In addition, the natural spin density obtained for $\mathbf{5}^+$ is localized on the ruthenium atom. From these results, [**Ru(III)**(N^-═$(NH_2)^+$)] is a good description for the electronic structure of $\mathbf{5}^+$. Considering the discussion on $\mathbf{5}^+$,

Chart 2. Electronic Structures of the Metal−Hydrazidium Bond

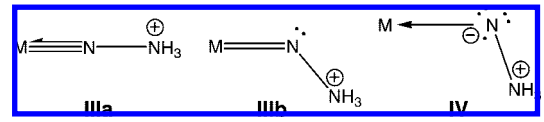

the electronic structure of $\mathbf{5}^0$ could be described as [**Ru(II)**(N^-═$(NH_2)^+$)]. The N_α−N_β and Ru−N_α distances of $\mathbf{13}^{+/0}$ are close to those of $\mathbf{5}^{+/0}$, while the total NPA charge on the N_2H_2 ligand is calculated to be +0.55 for $\mathbf{13}^+$ and +0.16 for $\mathbf{13}^0$. The electronic structures of $\mathbf{13}^+$ and $\mathbf{13}^0$ should be described as [**Ru′(II)**(N═$NH_2)^+$]] and [**Ru′(II)**(N^-═$(NH_2)^+$)], respectively.

4.4. Hydrazidium Complexes $\mathbf{6}^{+/0}$ and $\mathbf{14}^{+/0}$. To our knowledge, there are only a limited number of synthetic studies[54,55] on transition metal−hydrazidium complexes that can be compared with the present calculation probably because the N−N bond cleavage to give a metal−nitrido complex having a metal−nitrogen triple bond is thermodynamically favorable. All of the metal−hydrazidium complexes whose crystalline structures have been established possess a linear M−N−N structure[54] because of the contribution of the electronic structure **IIIa** in Chart 2. However, our result listed in Table 3 shows a significantly bent M−N−N structure for all hydrazidium complexes of the $RuIr_3S_4$ cluster and $[Ru(NH_3)_5]^{2+}$. While the NNH ligand in **4** and the NNH_2 ligand in **5** are located in the middle of the two nearest sulfur atoms in their optimized structures, the NNH_3 ligand in **6** occupies a position close to one of the two sulfur atoms (S^B in Figure 5). The H^A−S^B distance (2.617 Å) in $\mathbf{6}^+$ is much shorter than the H^A−S^A distance (2.868 Å) and is comparable to the Ir−H_A distance (2.670 Å). For neutral complex $\mathbf{6}^0$, the H^A−S^B, H^A−S^A, and Ir−H^A distances are calculated to be 2.656, 2.847, and 2.629 Å, respectively. The H−N−N−Ru structure of $\mathbf{6}^{+/0}$ implies that not only the Ir−H^A interaction but also the N_β−H^A−S^B hydrogen bond may stabilize the "reactive" NNH_3 ligand in the hydrazidium complexes. Both $\mathbf{6}^{+/0}$ and $\mathbf{14}^{+/0}$ have long N_α−N_β distances ranging from 1.500 to 1.533 Å, which are longer than the single N−N bond distance in hydrazine N_2H_4 (1.45 Å). The Ru−N_α distances in $\mathbf{6}^+$ (1.833 Å) and $\mathbf{14}^+$ (1.806 Å) are comparable to those in the imido complexes $\mathbf{8}^+$ (1.798 Å) and $\mathbf{8}^0$ (1.829 Å) but are much longer than that in the nitrido complex **7** (1.693 Å). Judging from the Ru−N distance and the bond order obtained by the NBO analysis, the Ru−N bond of $\mathbf{6}^+$ and $\mathbf{14}^+$ would have a double-bond character rather than a triple bond. The Ru−N_α distances in $\mathbf{6}^0$ (1.939 Å) and $\mathbf{14}^0$ (1.934 Å) are close to the value in [**Ru**(N_2)] **2** (1.948 Å). This indicates that the strength of the Ru−N bond in $\mathbf{6}^0$ and $\mathbf{14}^0$ are weaker than that in $\mathbf{6}^+$ and $\mathbf{14}^+$. The unpaired electron in $\mathbf{6}^0$ and $\mathbf{14}^0$ occupies the SOMO that is of antibonding between the Ru dπ and N_αp orbitals, leading the Ru−N bond weak in the neutral species. The small N_α−N_β−H angles (ca. 112°) indicate sp^3 character of N_β in all the hydrazidium complexes. The $N_\beta H_3$ moiety should be described as NH_3^+ because the total NPA charges on the $N_\beta H_3$ moiety were calculated to be +0.62 for

(54) (a) Galindo, A.; Hills, A.; Hughes, D. L.; Richards, R. L.; Hughes, M.; Mason, J. *J. Chem. Soc., Dalton Trans.* **1990**, 283. (b) Vale, M. G.; Schrock, R. R. *Inorg. Chem.* **1993**, *32*, 2767. (c) Retbøll, M.; Ishii, Y.; Hidai, M. *Organometallics* **1999**, *18*, 150.

(55) (a) Ishino, H.; Tokunaga, S.; Seino, H.; Ishii, Y.; Hidai, M. *Inorg. Chem.* **1999**, *38*, 2489. (b) Barclay, J. E.; Hills, A.; Hughes, D. L.; Leigh, G. J.; Macdonald, C. J. *J. Chem. Soc., Dalton Trans.* **1990**, 2503. (c) Retbøll, M.; Møller, E. R.; Hazell, R. G.; Jørgensen, K. A. *Acta Chem. Scand.* **1995**, *49*, 278.

$\mathbf{6}^+$, +0.60 for $\mathbf{6}^\mathbf{0}$, +0.34 for $\mathbf{14}^+$, and +0.25 for $\mathbf{14}^\mathbf{0}$. Assuming the double bond between the Ru atom and N_α, we can view the electronic structures of $\mathbf{6}^+$ and $\mathbf{14}^+$ as [**Ru(IV)**=N-$(NH_3)^+$] and [**Ru′(IV)**=N-$(NH_3)^+$], respectively, which correspond to structure **IIIb** in Chart 2. The Ru−N_α−N_β angle (112.4°) in $\mathbf{6}^\mathbf{0}$ is close to that of the sp^3 rather than the sp^2 N atom. The natural spin densities of $\mathbf{6}^\mathbf{0}$ and $\mathbf{14}^\mathbf{0}$ are delocalized on the Ru atom and N_α. Thus, the electronic structures of $\mathbf{6}^\mathbf{0}$ and $\mathbf{14}^\mathbf{0}$ would be regarded as [**Ru(II)**$(N^-−NH_3^+)$] and [**Ru′(II)**$(N^-−NH_3^+)$] (structure **IV**), respectively.

5. Conclusions

We performed DFT calculations on the cubane-type $RuIr_3S_4$ cluster, $[(CpIr)_3\{Ru(tmeda)(N_2)\}(\mu_3\text{-}S)_4]$ (**2**), to elucidate how dinitrogen is activated by complexation. Complex **2** is a model of the novel cubane-type mixed-metal sulfido cluster with an N_2 ligand, $[(Cp^*Ir)_3\{Ru(tmeda)(N_2)\}(\mu_3\text{-}S)_4]$ (**1**). The optimized structure of **2** reasonably reproduced the X-ray crystallographic structure of **1**. The elongated N−N bond distance, red-shifted N−N stretching frequency, and negatively charged N_2 ligand in **2** indicates that the N−N bond in **2** is reductively activated upon complexation. The degree of the N−N bond activation in **2** is classified into the "moderate activation" category, similar to Yandulov and Schrock's Mo−triamidoamine complex that can catalyze N_2 reduction. To discuss the N_2 reduction process mediated by the $RuIr_3S_4$ cluster, we investigated intermediates in a reaction pathway based on the Yandulov−Schrock cycle in detail. The calculated energy profile of the catalytic cycle demonstrates that the $RuIr_3S_4$ cluster is capable of serving as a catalyst for N_2 reduction in the presence of appropriate proton/electron donors (in the present case, $LutH^+/Cp^*_2Co$). Another interesting finding is the geometries of the intermediates having an NNH_x ($x = 1-3$) ligand. Complexes [**Ru**(NNH_x)] $\mathbf{4}^{+/0}$−$\mathbf{6}^{+/0}$ have a bent Ru−N−N structure, while metal−NNH_x complexes generally adopt a linear M−N−N structure. In particular, the diazenido complexes $\mathbf{4}^{+/0}$ favor a cis-bent Ru−N−N−H structure to a trans-bent structure. These unique geometries are reasonable considering the bonding interaction between a hydrogen atom bonded with the N_2 ligand and an iridium atom consisting of the cuboidal $RuIr_3S_4$ framework. In addition, noteworthy is that the Ru−N bond in $\mathbf{4}^{+/0}$−$\mathbf{6}^{+/0}$ tends to have a single-bond character, showing a contrast to a general tendency in metal−N_2 complexes that hydrogenations of the N_2 ligand intensify a multiple-bond character in the metal−N bond. The Ir−H interaction certainly plays a major role in the bent Ru−N−N structure in the $RuIr_3S_4$ cluster, and also a "loose" Ru−N bond would contribute to structural changes in the Ru−N−NH_x moiety.

Acknowledgment. This work was supported by Grants-in-Aid for Scientific Research (Nos. 18350088, 18066013, and 18GS0207) from the Japan Society for the Promotion of Science, the Global COE Project, the Nanotechnology Support Project of the Ministry of Education, Culture, Sports, Science, and Technology of Japan (MEXT), the Joint Project of Chemical Synthesis Core Research Institutions of MEXT, and CREST of the Japan Science and Technology Cooperation.

Supporting Information Available: Structural dependence of the Ru−N_2 complex on the basis set employed and the simplification of the bulky ligands are discussed in detail. Atomic Cartesian coordinates for all the structures optimized in the present study. This material is available free of charge via the Internet at http://pubs.acs.org.

JA8009567